Separation Science and Technology
Publication details, including instructions for authors and subscription information:
http://www.informaworld.com/smpp/title~content=t713708471

Performance of a Six-Port Simulated Moving-Bed Pilot Plant for Vapor-Phase Adsorption Separations

Giuseppe Storti[a]; Marco Mazzotti[b]; Luís Tadeu Furlan[b]; Massimo Morbidelli[b]; Sergio Carrà[b]
[a] DIPARTIMENTO DI CHIMICA INORGANICA, METALLORGANICA E ANALITICA UNIVERSITÀ DEGLI, PADOVA, ITALY [b] DIPARTIMENTO DI CHIMICA FISICA APPLICATA, POLITECNICO DI MILANO PIAZZA LEONARDO DA VINCI 32, MILANO, ITALY

To cite this Article Storti, Giuseppe , Mazzotti, Marco , Furlan, Luís Tadeu , Morbidelli, Massimo and Carrà, Sergio(1992) 'Performance of a Six-Port Simulated Moving-Bed Pilot Plant for Vapor-Phase Adsorption Separations', Separation Science and Technology, 27: 14, 1889 — 1916
To link to this Article: DOI: 10.1080/01496399208019456
URL: http://dx.doi.org/10.1080/01496399208019456

SEPARATION SCIENCE AND TECHNOLOGY, **27**(14), pp. 1889–1916, 1992

Performance of a Six-Port Simulated Moving-Bed Pilot Plant for Vapor-Phase Adsorption Separations

GIUSEPPE STORTI

DIPARTIMENTO DI CHIMICA INORGANICA, METALLORGANICA E ANALITICA
UNIVERSITÀ DEGLI STUDI DI PADOVA
VIA MARZOLO 1, 35131 PADOVA, ITALY

MARCO MAZZOTTI, LUÍS TADEU FURLAN,* MASSIMO MORBIDELLI,† and SERGIO CARRÀ

DIPARTIMENTO DI CHIMICA FISICA APPLICATA
POLITECNICO DI MILANO
PIAZZA LEONARDO DA VINCI 32, 20133 MILANO, ITALY

Abstract

A simulated moving-bed (SMB) pilot plant, characterized by two unique features, the number of ports (6 instead of 24, as in most industrial applications) and the fluid phase (vapor rather than liquid), has been built and operated. Such a plant has proven capable to achieve complete separation for a mixture of *m*- and *p*-xylene using isopropylbenzene as desorbent and KY zeolites as adsorbent. The dynamic behavior of the unit has been investigated and compared with model predictions, both in terms of approach to cyclic steady state as well as of responses to typical inputs. The role of the key design parameters on the steady-state separation performance of the unit has been analyzed experimentally, demonstrating the consistency with the predictions of the Equilibrium Theory.

1. INTRODUCTION

The adsorption separation of fluid mixtures based on displacement chromatography is most conveniently performed in a continuous unit where the solid and the fluid phases move countercurrently. With respect to the classical chromatographic approach, where several fixed-bed columns are operated in a cyclic batch mode, this unit is characterized by significantly

*On leave from PETROBRAS/CENPES/DIPOL, Cidade Universitaria, Quadra 7, Ilha do Fundao, 21910 Rio de Janeiro, Brazil.

†To whom correspondence should be addressed.

smaller solid and desorbent requirements (*1*). The scheme of a true countercurrent (TCC) unit of this type is presented in Fig. 1. Four external streams are shown: two entering (feed, i.e., the mixture to be separated; and fresh desorbent) and two leaving the unit (extract, enriched in the most adsorbable components; and raffinate, enriched in the least adsorbable ones). Four sections are evidenced, each one characterized by a specific role in the separation process. In particular, with reference to a binary mixture, the separation is performed in Sections 2 and 3, where the less adsorbable component is desorbed and the other one is adsorbed. Section 1 regenerates the adsorbent by desorbing the most adsorbable component, whereas Section 4 regenerates the desorbent by adsorbing the least adsorbable one.

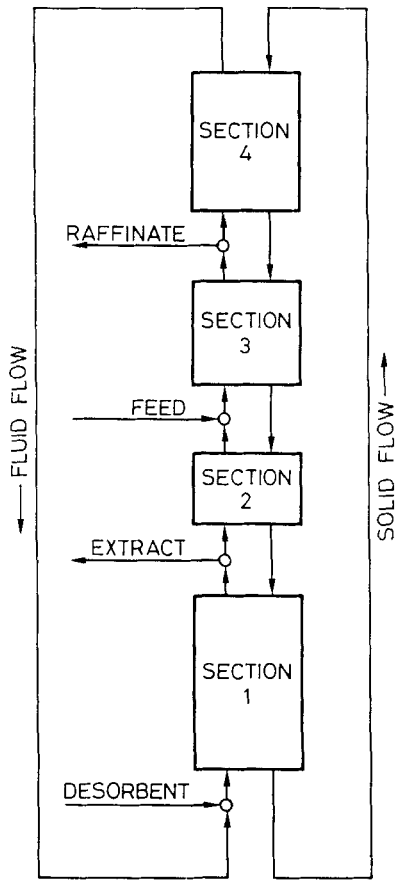

FIG. 1. Scheme of a four-section true countercurrent unit for adsorption separation.

The obvious problems related to the actual movement of the solid phase can be overcome by simulating this countercurrent contact by moving the fluid phase and the column in a fixed-bed unit. This column movement is produced by shifting the feed and withdrawal points along the column axis in the same direction as the fluid flow. In practice, this is obtained by discretizing each section of the unit into several ports or subsections; each one of these fixed beds is fed with the fluid stream leaving the previous subsection after addition or withdrawal of an external stream when required. A scheme of the simulated moving-bed (SMB) unit, which corresponds to the well-known SORBEX process developed by UOP (*2*), is shown in Fig. 2, where 12 subsections have been considered with port distribution (or configuration) 5-1-3-3.

In this work a pilot SMB unit has been built and tested. With respect to similar equipment previously reported in the literature, this apparatus has two unique characteristics:

1. The small number of ports (six)
2. The aggregation state of the fluid phase (vapor rather than liquid)

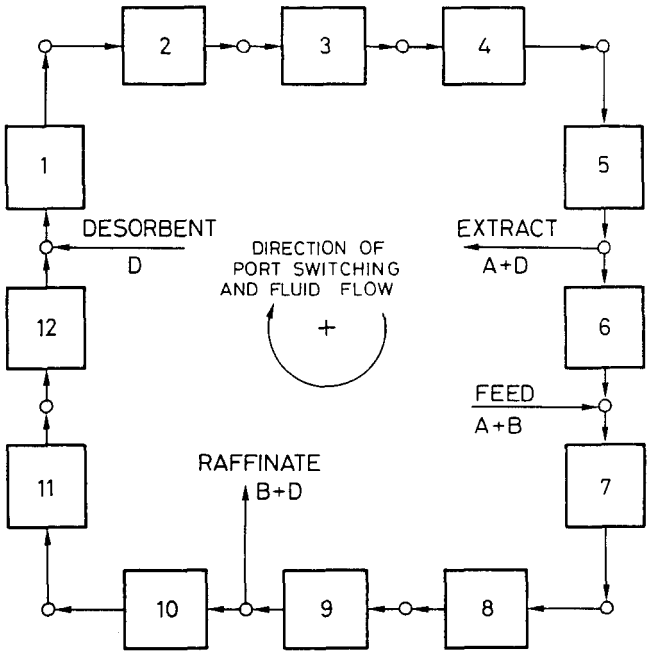

FIG. 2. Scheme of a 12-port simulated moving bed unit for adsorption separation (SORBEX).

In the following we focus on the analysis of dynamic behavior and steady-state separation performances rather than on the optimization of a specific separation process. The role of the key design parameters, i.e., the fluid–solid flow rate ratios, is examined both experimentally and theoretically as predicted by a simplified model based on equilibrium theory (*3*).

2. DESIGN OF THE SMB UNIT

The design of SMB units is usually performed with reference to a TCC unit (*4*), which is designed (in terms of fluid and solid flow rates, section length and diameter, and particle size) in the hypothetical case of a true countercurrent contact between the two phases. The equivalent design parameter values corresponding to the SMB unit are then determined so as to closely approach the separation performances of the equivalent TCC column. This is obtained through the following conversion rules between SMB and TCC:

$$\frac{L}{t^*} = \frac{u_s}{1 - \epsilon} \tag{1}$$

$$u_j^* = u_j + u_s \frac{\epsilon}{1 - \epsilon} \tag{2}$$

$$n_j L = L_j \tag{3}$$

where the parameters corresponding to the SMB unit and to the TCC one are reported in the left- and in the right-hand side, respectively, and j indicates the section index, being $1 \leq j \leq 4$.

These "conversion rules" follow from the geometric and kinematic equivalence between the two units. Thus, following the classical design approach, similar separation performances are expected when the port switching is made continuous, i.e., when the switching time interval t^* is reduced. According to the conversion rules, this leads to $L \to 0$ and $n_j \to \infty$, thus producing SMB units characterized by large values of the subsection number, $N = \Sigma n_j$. This is generally confirmed by industrial applications where at least three subsections per section are adopted, i.e., $N \geq 12$, while in most cases N is as large as 24.

The complexity of the SMB units designed as described above, which originates from the rather large number of ports, suggests the adoption of a different design procedure. This is based on the idea of taking rather large values of the port length L, so that the geometric equivalence (3) may be fulfilled with a low number of ports, i.e., 1 or 2 in each section.

Previously reported modeling results (5) indicated that rather modestly increased values of L are actually needed to obtain SMB units with a very low number of ports, say $N = 6$, which closely approach the separation performance of a TCC unit.

It should be noted that increasing values of the port length L lead to increasing values of the Stanton number, $St = k a_p L \epsilon / u$, and the Peclet number, $Pe = u d_p / \mathcal{D}_L \epsilon$, thus indicating that the SMB unit approaches its equilibrium behavior where mass transport resistances and axial mixing are negligible. In this case it can be shown (6) that, at least in the case where the desorbent adsorptivity is intermediate between that of the two components to be separated, the performance of the equilibrium SMB unit reproduces that of the corresponding equilibrium TCC unit. This leads to the design procedure of the SMB unit with a low number of ports. The flow rate values in each section are computed from the corresponding values in the equivalent equilibrium TCC unit through the kinematic equivalence conditions (1) and (2). Next, the value of the port length L is evaluated so that the SMB unit behavior closely approaches its ideal equilibrium behavior without reaching exceedingly high pressure drops. In this context the operation in the vapor phase should be preferred to that in the liquid phase since it is intrinsically characterized by larger mass transport efficiencies and lower axial mixing, i.e., larger values of St and Pe.

3. EXPERIMENTAL SET-UP

Let us describe the SMB pilot plant shown in Fig. 3 starting with the separation section, then illustrating the feeding and withdrawal zones. Next we illustrate the control system of the unit and the physical system adopted in the experiments, i.e., the mixture to be separated, the desorbent, and the adsorbent.

3.1. SMB Unit

The SMB separation unit is constituted of the columns where the separation takes place and the tubes and valves necessary to convey fluid streams and to perform port switches. All this apparatus is contained inside a thermostatic chamber capable of reaching a temperature of 300°C and keeping it uniform in space and constant in time with a maximum error of 1°C. This is a 600-L thermostatic chamber Modugral AB3BW1/S manufactured by Mazzali (Italy). During the experiments a little nitrogen stream is flowed through the chamber. It prevents air from entering the chamber and keeps its atmosphere inert by carrying away all possible leakages of organic species from the unit.

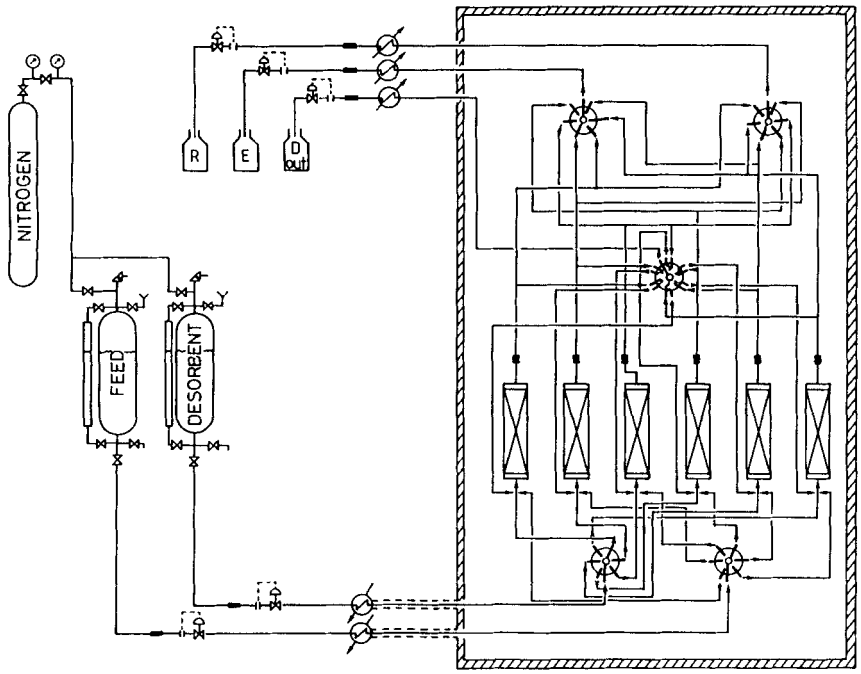

FIG. 3. Scheme of the experimental SMB pilot plant.

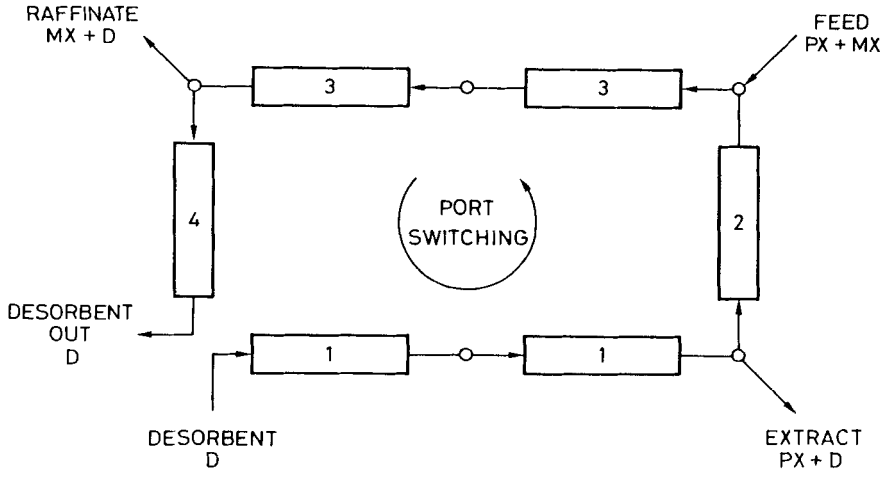

FIG. 4. Conceptual scheme of the 2-1-2-1 configuration of the SMB separation unit. Section number is indicated for each port.

A 2-1-2-1 configuration has been adopted, as shown in Fig. 4. This is because in the odd-numbered sections the flow rate is greater than in the even-numbered ones and consequently the approach to equilibrium conditions is disfavored. This can be compensated for by longer sections, hence the chosen configuration is appropriate to give balanced conditions to each section with respect to the approach to equilibrium. All the experimental runs reported in this paper have been performed with the separation unit configuration 2-1-2-1.

We have adopted an open loop process in which the stream coming out of the fourth section is not recycled to the first section but is collected. Thus, in order to reproduce the behavior of the closed loop scheme shown in Fig. 2, the flow rate of the desorbent stream fed to Section 1 is equal to the sum of the fresh desorbent and the recycle stream in Fig. 2. It must be pointed out that the open loop process is equivalent to the closed loop one provided that the outgoing desorbent stream is pure. All the experimental runs discussed in this paper fulfill this condition.

Each port is a 120-cm long stainless steel column (15 mm internal diameter). The adsorbent solid fills 100 cm of each column, the other 20 cm being stuffed with glass wool for the purpose of properly distributing the inlet flow and of retaining the solid particles carried by the outlet fluid. As an extra protection a Swagelok filter, with a sintered element of 7 μm size, is located at the outlet of each column.

The port switching, which simulates the fluid–solid countercurrent movement, is performed by four 6+1 port 6-position valves and one 12+1 port 6-position valve, as shown in Fig. 3.

Two of the 6+1 port valves are used to convey the feed and the desorbent streams to each of the six column inlets, while the other two connect each column outlet to the extract and raffinate reservoirs. The 12+1 port valve is instead used to connect each column outlet to the inlet of the following column, except for one which is, at the proper switching time, connected to the reservoir of the outgoing desorbent.

The five multipositional valves are chromatographic valves manufactured by Valco Instruments Co. (USA), models E6SD6T and E6SF6T. They can work at a maximum temperature of 300°C with an operating pressure limit of 200 psi. Each valve is electrically actuated, and it is connected to the actuator by a specially designed 45 cm long stand-off which passes through a hole in the wall of the thermostatic chamber. The part of the stand-off outside the chamber is cooled by means of a water coil in order to keep the actuator below an operating temperature of 50°C.

All the lines in the hot section of the plant are made of 1/8″ stainless steel tubes. The fittings that connect the lines to the valves are made by VICI, whereas all the others are stainless steel Swagelok fittings.

3.2. SMB Pilot Plant

Fresh desorbent and feed are stored as liquids in reservoirs consisting of two tanks each, one being the back-up of the other. Tanks are kept under constant pressure with nitrogen and equipped with a relief valve.

The flow rates of the fresh desorbent and of the feed stream are controlled in the liquid state through a mass flowmeter and controller (model F912-FA-11-LFC, manufactured by Bronkhorst HIGH-TECH B.V., The Netherlands). The control system is virtually independent of pressure and temperature, but it needs a minimum pressure drop of about 1 bar for the control valve to work properly. After this the streams are vaporized and then enter the thermostatic chamber containing the SMB unit where each stream is led to the relevant multipositional valve.

Three streams come out of the chamber. They are first condensed in simple tube-tube heat exchangers, and then they are metered and controlled by three liquid flow control systems identical to those mentioned above. Since the liquid flow control systems have a pressure drop of about 1 bar and the collecting tanks are at atmospheric pressure, the pressure in the unit must be at least 2 bar. Sampling points (not shown in Fig. 3) are positioned after the mass flow meters and controllers so as to avoid any perturbation of the flow rates in the separation section during sampling.

All lines in the cold section of the pilot plant are made of 1/8" copper tubes, connected by brass Swagelok fittings.

3.3. Control of the Unit

With reference to the open loop configuration shown in Fig. 4, seven overall mass flow rates must be given a value in order to uniquely establish the steady-state operation of the SMB unit. These are the mass flow rates in Sections 1 and 4—which coincide with those of fresh and outgoing desorbent, respectively—the mass flow rates in Sections 2 and 3, and the mass flow rates of extract, raffinate, and feed. There are only three relationships among the seven variables, i.e., the overall material balances at the extract, raffinate, and feed nodes. Hence, four degrees of freedom are left and must be constrained in order to fully determine the system and achieve the desired operating conditions.

In principle it would be sufficient to control four mass flow rates, e.g., mass flow rates of fresh desorbent, feed, extract, and raffinate streams, thus leaving the last output stream free. In practice, we also need to control the pressure value in the unit, which, as mentioned above, should exceed the minimum value of 2 bar required by the proper operation of the unit. This can be achieved very conveniently by introducing a fifth liquid flow controller on the outgoing desorbent stream.

In the start-up of the unit the separation columns are loaded with the fluid mixture while keeping the outgoing lines closed until the desired pressure level is reached. Then all the mass flow controllers are set to the operating values, which obviously fulfills the overall material balance of the unit, and the separation process is started. During the operation of the unit, the set-points of all the mass flow controllers are kept constant, except for the fifth one (on the outgoing desorbent stream) whose set-point is continuously adjusted in order to keep the pressure value in the unit constant. This control loop is very efficient in keeping the unit at stationary conditions, since small errors in the flow rates of the inlet or outlet liquid streams produce an accumulation of material in the unit which is immediately evidenced by a pressure increase.

3.4. Experimental System

The experiments described in this paper deal with the separation of an equimolar mixture of *m*-xylene and *p*-xylene (51% *m*-X, 49% *p*-X), using isopropylbenzene as desorbent. The adsorbent is constituted of 1/16″ pellets of KY zeolite. In this case the adsorptivity of the desorbent is intermediate with respect to those of the components to be separated, i.e., the weak component which is *m*-xylene and the strong one which is *p*-xylene.

The experimental samples were analyzed by means of a Carlo Erba Strumentazione gas-chromatograph equipped with an FID detector.

4. ANALYSIS OF THE DYNAMIC BEHAVIOR OF THE UNIT

The operating regime of the SMB unit is intrinsically time-dependent. Each column of the separation unit goes through a transient during each time period between two port switches. The dynamics starts at the port switching time with initial conditions given by the state of the column at that moment, and develops until the next port switch ending at a final state which is the initial state for the next time period. The developing of concentration traveling waves in the columns during each time period has its counterpart in the nonconstant time concentration profiles at the withdrawal points of the unit. Accordingly, we can identify for each column a dynamic behavior with a time scale equal to the switching time t^* (time period between two port switches), which superimposes to the slower dynamics of the overall unit that begins at the start-up of the plant and lasts until cyclic steady-state conditions have been achieved. This stationary regime is characterized by a periodic behavior of each physical column with a period equal to the switching time multiplied by the number of ports (t^*N). This is the cyclic steady-state of the SMB unit, which is the one of interest in applications where the time average concentrations in the with-

drawal streams are constant. It must be pointed out that under these conditions the instantaneous concentrations in the output streams have a period equal to t^* that corresponds to the period of each "logical" column (defined as the column that performs the same task during each time period).

In the following we address the issue of the achievement of cyclic steady-state by first introducing the criteria used to identify cyclic steady-state conditions of the pilot plant. Next, we investigate the slow dynamics that drives the system during the overall transient from start-up to cyclic steady state, with specific reference to the time to reach cyclic steady state (t_{ss}). A comparison between numerical and experimental results obtained for liquid-phase and vapor-phase operations is illustrated. Eventually the analysis of the dynamic behavior of the unit is completed by considering the responses to typical inputs, such as a step change in the set-point or a disturbance in the operating conditions.

4.1. Achievement of Cyclic Steady-State Conditions

4.1.1. Adopted Criteria to Identify Cyclic Steady-State

The analysis of the separation performance of the SMB pilot plant must be done with reference to the stationary regime of the unit. Since the behavior of the unit is always time-dependent, it is necessary to use reliable criteria to identify the stationary regime, i.e., the cyclic steady-state. The three criteria we have adopted are described in the following.

Constant Average Concentration in Extract and Raffinate. The average concentration values in the output streams—extract, raffinate, and outgoing desorbent—are supposed to remain constant after the unit has reached cyclic steady-state. Monitoring the concentration values in the output streams averaged over the switching time period t^* gives an illustration of the overall dynamics of the unit, both in the case of the start-up transient as well as in the case of the response to various disturbances. When the values of these concentrations are constant except for minor fluctuations, it is assumed that the cyclic steady-state has been reached. It must be pointed out that these quantities are precisely what is needed to determine the steady-state separation performance of the pilot plant.

It is worth noting that the concentration values mentioned above are time averages obtained by collecting the output streams for the time period between two port switches. Whenever the sample collection is begun with respect to the port switching time, once cyclic steady-state conditions are reached, the measured average concentration values remain constant, provided that the collection period is equal to t^*. We assume that the stationary

regime has been reached when the relative differences in the values of the average concentrations are less than 5%.

In Fig. 5 the time-average concentration profiles of *p*- and *m*-xylene in extract and raffinate are shown. It can be seen that in this experimental run complete separation has been obtained, while the concentration profiles clearly show the start-up transient and the achievement of cyclic steady-state. The fluctuations present in the experimental data are likely to be due to several different reasons: gas chromatographic analysis errors, fluid dynamics irregularities, nonreproducibility of the sampling procedure. The value of 5% as a maximum relative error has been chosen as a conservative estimate of the combined effect of all such uncertainties.

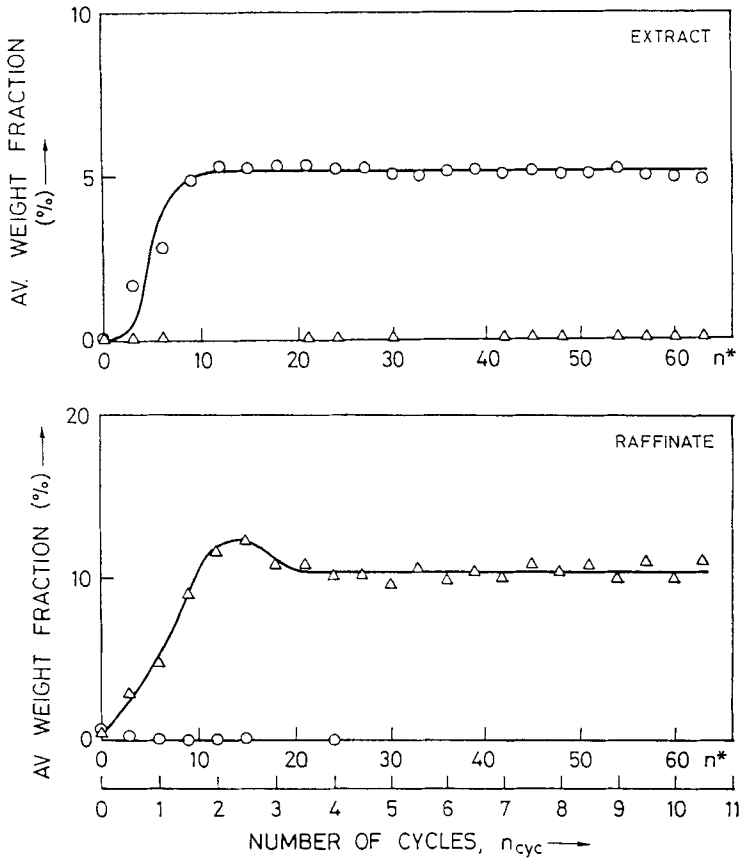

FIG. 5. Average concentration profiles in extract and raffinate during Run A (see Table 2): $t^* = 6$ min, (Δ) *m*-xylene, (○) *p*-xylene.

Fulfilment of Overall Mass Balance and Single Component Mass Balances. The criterion described above is a necessary condition for the achievement of cyclic steady-state, not a sufficient one.

The criterion of constant average concentrations must be coupled with a criterion related to the fulfilment of the material balances of the unit, so as to indicate that there is no accumulation in the unit. In particular, we consider both the overall material balance and the single component material balances, and we verify that mass flow rates going in are equal to mass flow rates coming out of the unit. It should be noted that single component material balances are much more sensitive than the overall material balance.

For single component material balances, computed with the values of mass flow rate and concentration measured during the same time period, a relative error between ingoing mass flow rates and outcoming ones of about 2% is considered acceptable.

The absence of accumulation inside the unit coupled with constant average concentrations in the output streams provides necessary and sufficient conditions for the achievement of cyclic steady-state.

Periodic Behavior of Instantaneous Concentration Profiles in Extract and Raffinate. When both the criteria described above are satisfied, the unit is in the stationary regime. As a further proof of this we can verify that the instantaneous concentration profile at the withdrawal points is indeed periodic. To this aim we measured them during different time periods when the unit is supposed to be in the stationary regime according to the previous criteria. If the obtained concentration profiles are identical within the experimental error, the behavior of the unit is definitely periodic. The monitoring of the instantaneous concentration has been done by sampling the output streams several times during one time period (of length t^*). The measured instantaneous concentration is in fact an average concentration over a short time (~20 s), long enough to collect the minimum quantity of fluid required by the analytical procedure but much shorter than the time period t^*.

In Fig. 6 the average concentration profiles obtained during Run B are shown. The operating conditions were deliberately chosen so as to obtain no separation. At times indicated by a and b, about 2 hours apart, an instantaneous sampling was performed. The instantaneous concentration profiles are shown in Fig. 7 where it can be seen that profiles obtained at times a and b are in excellent agreement.

Time 0 in Fig. 7 corresponds to the first port switch, and Time 8 corresponds to the next port switch. Due to the presence of a relevant dead volume between the exit of the columns and the sampling points, there is a time lag between the output of the columns and what is actually collected at the sampling points. As a consequence, the concentration profiles shown

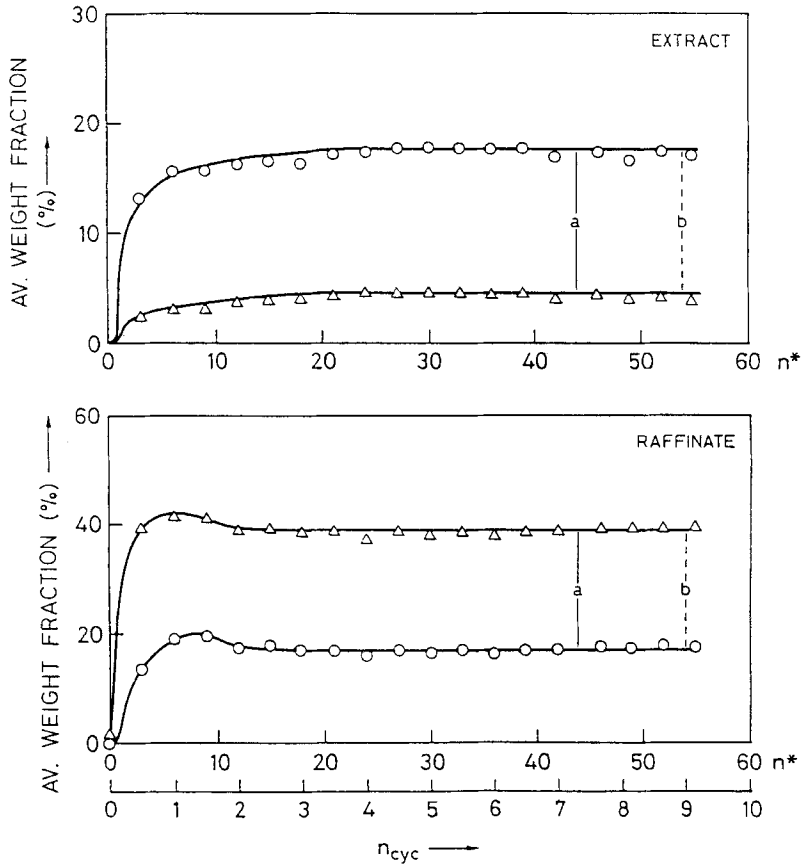

FIG. 6. Average concentration profiles in extract and raffinate during Run B (see Table 2): t^* = 8 min, (Δ) *m*-xylene, (○) *p*-xylene, (*a*) first instantaneous sampling, (*b*) second instantaneous sampling.

in Fig. 7 must be shifted horizontally by a quantity equal to the time lag to obtain the actual concentration profiles at the outlet of the columns. The time lags indicated in the caption of the figure are estimates. They are different for the extract and the raffinate because the dead volume is roughly the same but the flow rates are not. It must be pointed out that back-mixing can have an important role in the dead volume, in particular along the tube-tube condenser where not only axial diffusion but also macromixing is present. Therefore the true concentration profiles at the outlet of the columns are supposed to be sharper and steeper than the ones shown in Fig. 7.

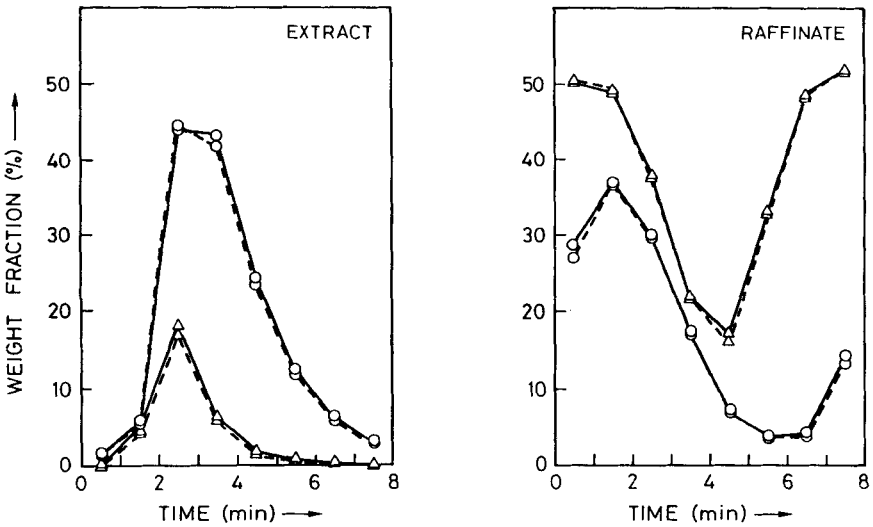

FIG. 7. Instantaneous concentration profiles in extract and raffinate during Run B (see Table 2): $t^* = 8$ min, (Δ) *m*-xylene, (○) *p*-xylene, (——) profile at time *a*, (– –) profile at time *b*, time lag in extract: 1'50", time lag in raffinate: 2'55".

4.1.2. Transient Behavior

Once satisfactory criteria to identify the achievement of cyclic steady-state are defined, let us analyze the system behavior during the transient from the start-up of the unit to the stationary regime. This analysis must be done with reference to the average concentrations in extract and raffinate, which characterize the overall slow dynamics of the unit.

In particular, we are going to consider the time to reach cyclic steady-state, t_{ss}, i.e., how long it takes for the unit to get to the stationary regime, and the behavior of the unit during the transient period, i.e., what the time concentrations profiles look like during the transient period. Both of them are discussed by comparing calculated and experimental results for liquid- and vapor-phase operation.

Calculated values of the time to reach cyclic steady-state t_{ss} for a six-port SMB unit are shown in Fig. 8 as a function of the switching time t^*. The value of t_{ss} has been determined as the time when the ratio between the average concentration and the cyclic steady-state concentration becomes equal to 0.99. The results obtained indicate that the number of port switches needed to reach cyclic steady-state ($n_{ss}^* = t_{ss}/t^*$) is indeed independent of the switching time and is given by the slope of the straight line shown in Fig. 8. It can also be seen that the values of n_{ss}^* so obtained, as

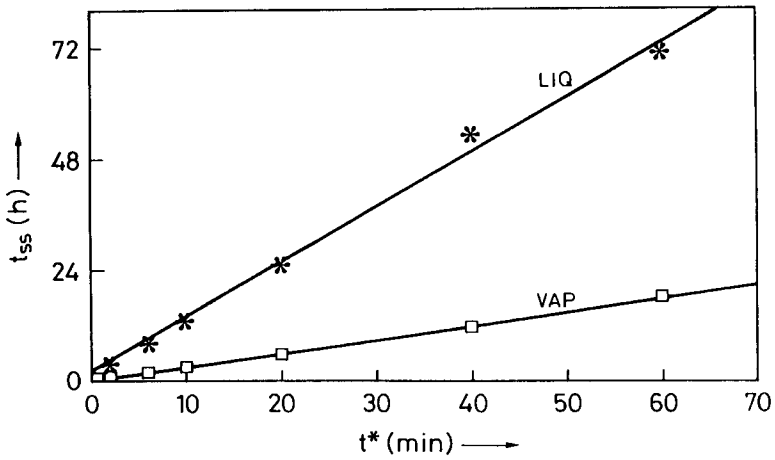

FIG. 8. Calculated values of time to reach steady-state, t_{ss}, as a function of the switching time t^* for the six-port SMB unit and a typical system: (*) liquid-phase operation, (□) vapor-phase operation.

reported in Table 1, are largely different for the vapor-phase and the liquid-phase operation. With the physical parameters used to perform the calculations, the number of port switches to reach cyclic steady-state in the liquid phase is about four times the same number for the vapor phase.

Let us now analyze the unit behavior during the transient by considering the ratio between the actual and the steady-state concentration values c/c_{ss} of *p*-xylene in the extract as a function of the number of cycles shown in Fig. 9. It should be stressed that the broken curves shown in Fig. 9 actually represent all the transients considered in Fig. 8, corresponding to different values of the switching time, t^*, both for liquid- and vapor-phase operation. This is because all concentration profiles are brought together

TABLE 1
Number of Switches (n_{ss}^*) and Number of Cycles (n_{ss}^{cyc}) to Reach Steady-State

	N	n_{ss}^* calc.	n_{ss}^{cyc} calc.	n_{ss}^* exp.	n_{ss}^{cyc} exp.	Reference
Vapor	6	18	3	18 ÷ 24	3 ÷ 4	This work
	12	30	2.5	—	—	
Liquid	6	72	12	—	—	
	12	120	10	—	—	
	24	—	—	240	10	7

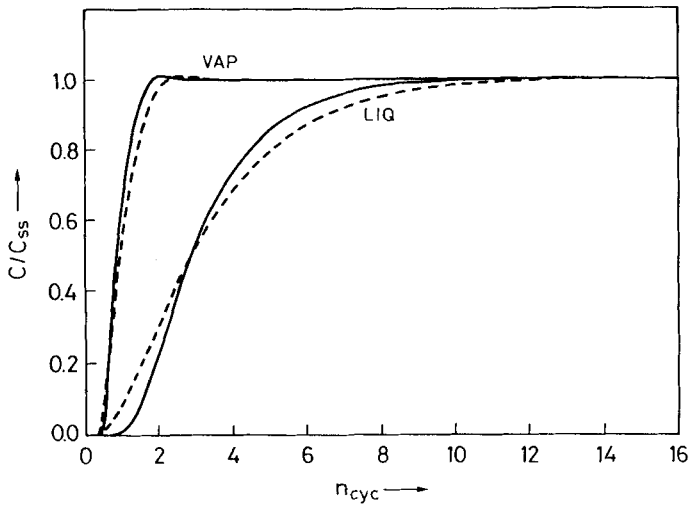

FIG. 9. Normalized concentration profile c/c_{ss} of *p*-xylene in extract as a function of the number of cycles: (——) 12-port unit, (– –) 6-port unit.

when concentration is normalized with respect to the steady-state value and time is scaled by t^*. Moreover, in the same Fig. 9 the results referring to two values of the number of ports N are also shown, i.e., $N = 6$ for the broken curve and $N = 12$ for the solid curve. It is also seen that these curves are actually brought together by the selection as the independent variable of the number of cycles, $n^{cyc} = t/(Nt^*)$. This indicates that the time scale for describing the transient of SMB units is the number of cycles. This is confirmed by the results reported in Table 1 where it appears that the value of n_{ss}^{cyc} needed to reach steady-state independently of the number of ports in the unit is about 3 for the vapor-phase operation and 10 for the liquid-phase one. These values are in satisfactory agreement with the experimental findings.

This result can be interpreted in terms of the renewal time ratio between the liquid- and the vapor-phase operation. The renewal time of the unit is defined as the ratio between the unit hold-up and the total flow rate entering the unit. The hold-up is given by the sum of the hold-up in the adsorbed phase, which for the system under examination is about the same in both cases, and the hold-up in the fluid phase, which is proportional to the density of the fluid phase itself ($\rho_L/\rho_V \simeq 100$). Considering the same inlet flow rate, the renewal time ratio becomes equal to the ratio between liquid hold-up and vapor hold-up. This ratio can be approximated by $[\rho_L/(\rho_s\Gamma^\infty) + 1]$, which for the system under examination is approxi-

mately equal to 4. It is worth noticing that this estimate, though based on overall steady-state properties, is very similar to the ratio between the number of cycles to reach steady-state in the liquid- and in the vapor-phase operation.

4.2. Response of the Unit to Typical Inputs

In the following the dynamic responses of the SMB unit to some typical inputs are investigated. This analysis is meant to verify the correctness of the results obtained in the previous section regarding the time scale of the transient from start-up to cyclic steady-state. Furthermore, the effect of start-up conditions on the overall dynamics of the unit is discussed.

4.2.1. Effect of Start-up Conditions

The initial conditions at the start-up of the SMB separation unit have a strong effect in determining the time behavior of the average concentrations at the withdrawal points, together with the values of the mass flow rates in the different sections, which are also responsible for the steady-state performance of the separation unit. Some examples of concentration profiles during the transient from start-up to cyclic steady-state are shown in Figs. 5, 6, and 10–13. Let us analyze the behavior of the raffinate concentration (with similar comments being applicable to the extract concentration profile).

It is worth considering that at the beginning of the experiment each component is carried by the phase (fluid or solid) in which it preferentially stays at about the same velocity as the phase itself. As a consequence, *m*-

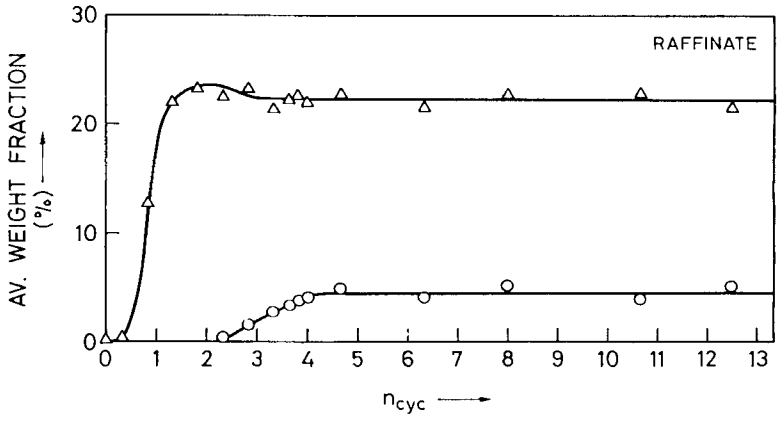

FIG. 10. Average concentration profiles in raffinate during Run C (see Table 2): t^* = 10 min, (Δ) *m*-xylene, (○) *p*-xylene.

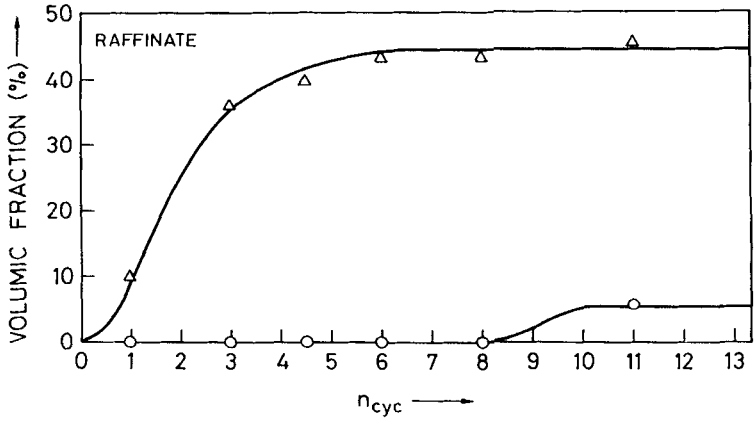

FIG. 11. Average concentration profiles in raffinate from Fig. 15a in Ref. 7: $t^* = 20.45$ min, (Δ) *m*-xylene, (○) *p*-xylene.

xylene, the least adsorbable compound, appears in the raffinate a few valve switches after start-up, and its concentration reaches a level close to the steady-state concentration after one or two complete cycles of valve switches. This appears rather clearly in Figs. 5, 6, and 10–12, where at the beginning of the experimental run the unit was filled with the desorbent. On the other hand, if at the beginning the raffinate zone of the unit, i.e., Sections 3 and 4, is filled with a mixture of the three species, as it is in the case of the experimental run shown in Fig. 13, then *p*-xylene is carried by the solid phase away from the raffinate at the velocity of the solid itself. This justifies the initial drop of *p*-xylene concentration in the raffinate shown in Fig. 13.

The extent at which each component is carried by the phase in which its presence is not favored is strongly dependent on the operating conditions of the unit, and particularly on the values of the mass flow rates in each section. These have a strong influence on the concentration profiles during the transient, which can be clearly evidenced by comparing Figs. 6 and 10. In both cases the operating conditions determine poor separation, but the undesired component (*p*-xylene in the raffinate) shows up very early during Run B in Fig. 6, whereas it appears more than two complete cycles after start-up during Run C in Fig. 10.

The situation illustrated in Fig. 10 can be considered an extreme case in which the most adsorbable component appears in the raffinate after a number of cycles close to that needed to reach cyclic steady-state. This behavior can be understood by considering the spatial concentration pro-

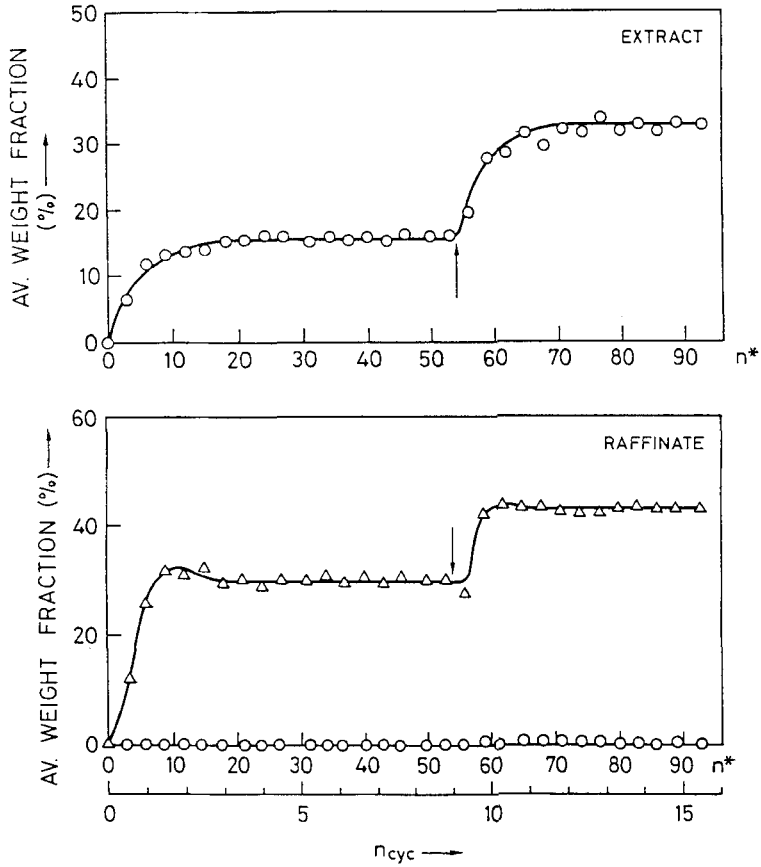

FIG. 12. Average concentration profiles in extract and raffinate during Run D (see Table 2): $t^* = 6$ min, (Δ) *m*-xylene, (○) *p*-xylene. Arrows indicate the change in the set point.

files inside the columns. They are approximately constituted of constant states separated by smooth transitions (*8*) which travel in space in the same direction as the fluid flow but at different velocities. The operating conditions can be such that in the column preceding a withdrawal point a constant concentration plateau is present and the transition following it is far from the exit of the column but a little faster than the fluid flow rate. If this happens, almost constant average concentrations are observed initially in the output stream, and only after a considerably great number of port switches does the transition show up at the withdrawal point, bringing about a change in the relevant average concentrations. Accordingly, the transient behavior of the unit shown in Fig. 10 is readily explained con-

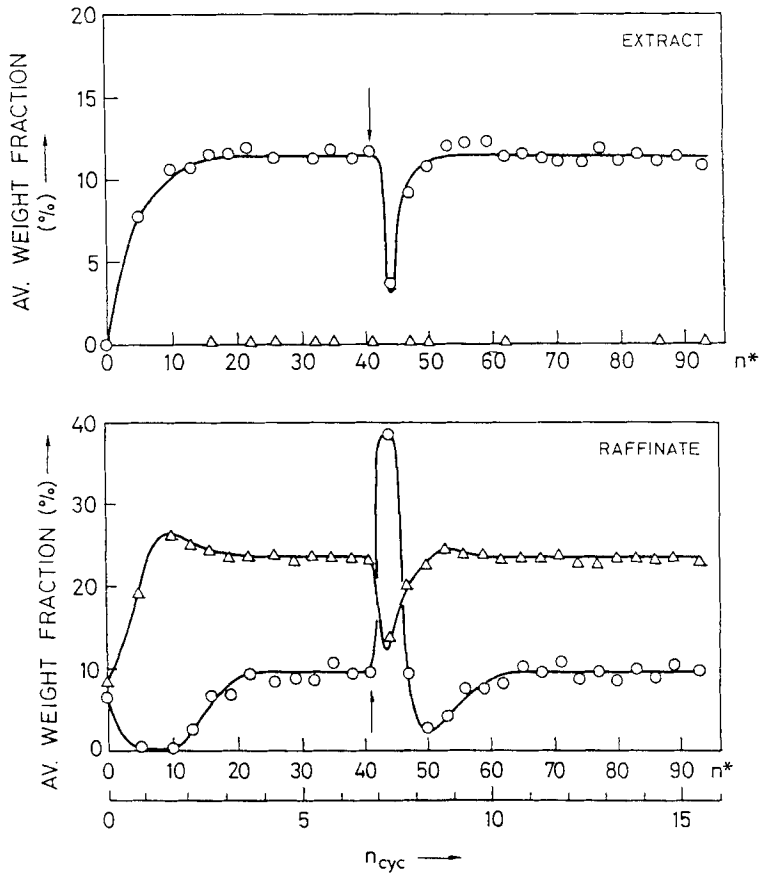

FIG. 13. Average concentration profiles in extract and raffinate during Run E (see Table 2): $t^* = 6$ min, (Δ) *m*-xylene, (○) *p*-xylene. Arrows indicate the occurrence of the disturbance.

sidering that the constant state traveling in front of the transition has zero concentration of *p*-xylene.

The results presented by Balannec and Hotier (*7*) and shown in Fig. 11 can possibly be interpreted in the same way. These refer to the liquid-phase separation performed in an SMB unit with 24 columns of about the same dimension as the columns used in our pilot plant. In this case *p*-xylene reaches its steady-state concentration only after about 10 cycles, which corresponds to an elapsed time from start-up of about 82 hours.

4.2.2. *Response to a Step Change in the Set Point*

The concentration profiles shown in Fig. 12 correspond to an experimental run (D in Table 2) where a step change was given to the operating

TABLE 2
Operating Conditions and Performances of the Experimental Runs

	Mass flow rate ratio				Extract (wt%)		Raffinate (wt%)		Purity (%)	
Run	m_1	m_2	m_3	m_4	*p*-X	*m*-X	*p*-X	*m*-X	P_E	P_R
F	**3.583**	**0.798**	**1.167**	**0.379**	6.5	<0.02	<0.02	23.0	>99.7	>99.9
G	3.583	**0.655**	1.146	0.409	8.5	1.0	<0.02	29.0	89.5	>99.9
C	3.583	**0.850**	1.249	0.368	6.0	<0.02	4.0	22.0	>99.6	84.6
B	2.858	**0.589**	**1.900**	0.434	17.0	4.0	17.5	39.0	81.0	69.0
H	**2.518**	0.809	1.177	**0.501**	10.0	<0.02	<0.02	27.0	>99.8	>99.9
J	**2.057**	0.796	1.216	**0.529**	16.0	<0.02	0.1	30.0	>99.9	99.7

conditions of the unit. It appears that the unit reaches a first cyclic steady-state after about three cycles of valve switches, which corresponds to a very good separation. At the ninth cycle (indicated by an arrow in Fig. 12) a step change is given to the mass flow rate set points in Sections 1 and 4. In particular, the mass flow rate in Section 1 is decreased, whereas the mass flow rate in Section 4 is increased. As a consequence, the net mass flow rate of desorbent decreases and the concentrations of *p*- and *m*-xylene in extract and raffinate increase. Because of the careful choice of the new set points, the separation remains good, as illustrated in the figure.

It is worth pointing out that the transient from the first to the second stationary regime is very similar to the transient following the start-up of the unit. In both cases the system takes the same time (about three cycles) to achieve the stationary regime.

4.2.3. Response to a Disturbance in the Operating Conditions

A behavior having the same time scale as the one discussed above is expected when a pulse disturbance enters the system. In this case, since the cyclic steady-state is stable and the operating conditions after the disturbance return to the preceding values, the unit recovers the same stationary state.

During the experimental run shown in Fig. 13, a sudden increase of pressure in the first section occurs. The disturbance does not propagate to downstream sections because the pressure drop is concentrated in the first section (due to the highest mass flow rate) and the operating pressure is soon recovered after the pulse. The system is already in the stationary regime when the disturbance occurs, almost at the completion of the seventh cycle (as indicated by an arrow in Fig. 13). It supposedly causes

condensation of *p*-xylene in the first section, followed by transfer of condensed *p*-xylene to the fourth section at the moment of the successive valve switch. This interpretation of the phenomenon is consistent with the sudden increase of *p*-xylene concentration in the raffinate and the contemporary decrease in the extract.

In all cases, in this context it is important to remark that the time needed by the unit to recover the steady-state conditions is again equal to about 3 cycles.

5. ANALYSIS OF THE ROLE OF THE DESIGN PARAMETERS ON THE SEPARATION PERFORMANCE

The key design parameters of an SMB unit as determined by Equilibrium Theory (*8*, *9*) are the ratios between the net fluid mass flow rate and the adsorbed phase mass flow rate in each section of the unit. The net fluid flow rate is evaluated as the difference between the fluid flow rate and the backmixed portion of it, due to the fluid carried by the solid inside the macropores, which has a detrimental effect on separation. In terms of the variables of the equivalent TCC unit, the mass flow rate ratios in each section are defined as follows:

$$m_j = \frac{\text{net fluid flow rate}}{\text{adsorbed phase flow rate}} = \frac{u_j\rho_f - u_s\epsilon_p\rho_f}{u_s\rho_s\Gamma^{\infty}(1 - \epsilon_p)} \tag{4}$$

At this stage both mass transport resistances and axial mixing are neglected; thus, a "thermodynamic" design is performed, properly accounting for the adsorption nonlinearities with reference to constant selectivity, stoichiometric systems. Once these ratios are evaluated, the absolute fluid velocity field is determined so as to fit the admissible range of pressure drop and minimum mass transport resistances for the given column length and particle size. The operating conditions for the SMB unit are obtained from those for the TCC unit through the kinematic equivalence (1) and (2) (*6*, *9*).

It is worth pointing out that if complete separation is desired, the value of each flow rate ratio m_j must be chosen within a given interval. Special limits are the lower bound for m_4 which is zero and the upper bound for m_1 which is ∞. At one of the two bounds of the interval, optimal conditions in terms of solid and desorbent requirements are obtained, but the robustness of the operation is minimal, i.e., if the operating conditions are slightly perturbed, the separation performance drops dramatically. By moving away from the optimal bound, the separation is still complete with higher solid and desorbent requirements, but the robustness of the operation increases (*9*).

The operating conditions, the steady-state parameters, and the performance of the experimental runs are reported in Table 2.

Among them, Run F, whose operating conditions correspond to complete separation and good robustness, is chosen as the reference case with which the others are compared. The 0.02% value in the table represents the least detectable concentration of xylenes in the samples. Hence "<0.02%" means that the presence of that component was not detected by the analysis and represents the upper value for its concentration. The relevant lower bound for purity is calculated on this upper value.

In the following the experimental results are analyzed by considering the effect of a change in one or two flow rate ratios at a time. The other flow rate ratios remain constant, with values very close to the reference case, hence ensuring separation as far as they are concerned. The experimental runs illustrating the effect under consideration are taken from Table 2, and their results are discussed and compared with the equilibrium theory predictions. This comparison is performed in a qualitative fashion because a complete characterization of the properties of the adsorbent with respect to the mixture of xylenes and isopropylbenzene used in the experiments is still lacking at this stage.

5.1. Effect of Mass Flow Rate Ratio m_2 on the Purity of Extract and Raffinate

As explained in the Introduction, the role of Section 2 is to desorb *m*-xylene, the least adsorbable compound. It follows that if m_2 is decreased below a lower limit value, a loss of purity in the extract is observed. On the contrary, increasing m_2 above the reference value has no negative effect on extract purity, but lowers the concentration of *p*-xylene in the extract itself, i.e., the enrichment of the extract.

When the value of m_2 is increased above an upper limit value, not only all the *m*-xylene but also a great amount of *p*-xylene is desorbed. This quantity is too much for Section 3 to adsorb and, as a consequence, raffinate purity drops.

All these effects are predicted by Equilibrium Theory. In Fig. 14 the calculated behavior of extract and raffinate purities is shown, and the existence of bounds on the flow rate ratio in Section 2 to obtain complete separation is demonstrated.

The same behavior is observed by considering the experimental Runs G and C, together with the reference Case F, in Table 2. In the reference case, complete separation is achieved: neither *m*-xylene in the extract nor *p*-xylene in the raffinate are detected. In Run G, m_2 is decreased and extract purity is lost while raffinate purity is still complete. In Run C, m_2 is increased and, as expected, the opposite effect is observed.

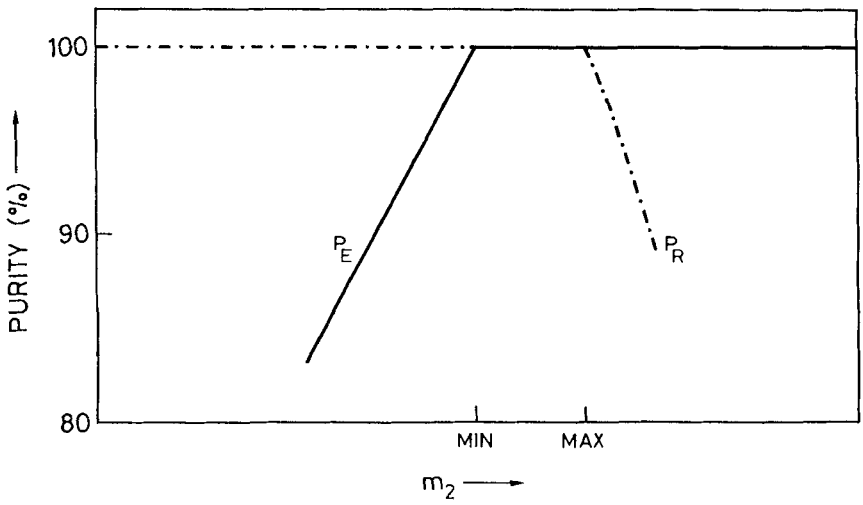

FIG. 14. Extract (P_E) and raffinate (P_R) purity values as a function of the mass flow rate ratio in Section 2 as predicted by the Equilibrium Theory.

5.2. Combined Effect of Mass Flow Rate Ratios m_2 and m_3 on the Purity of Extract and Raffinate

The role of Section 3 is to adsorb *p*-xylene, the most adsorbable component. This is achieved if the solid flow rate is high enough, i.e., if the flow rate ratio is sufficiently low. It follows that the change of m_3 has the same qualitative effect as the change of m_2 described above. This is shown in Fig. 15 where the purity values predicted by the Equilibrium Theory in extract and raffinate are reported as a function of the flow rate ratio in Section 3.

The loss of raffinate purity caused by the increase of m_3 is observed in experimental Run B in Table 2, where this effect is combined with the decrease of m_2 with respect to the reference Case F. As discussed above, the latter change causes the drop of extract purity.

5.3. Combined Effect of Mass Flow Rate Ratios m_1 and m_4 on the Enrichment in Extract and Raffinate

As explained in the Introduction, Sections 1 and 4 are responsible for the regeneration of the adsorbent and of the desorbent, respectively.

The flow rate ratio in Section 1 must be high enough to desorb all *p*-xylene from the adsorbed phase. If this is not the case and m_1 decreases below its lower limit value, some *p*-xylene remains adsorbed and is taken to Section 4 after the next valve switch and to Section 3 after another

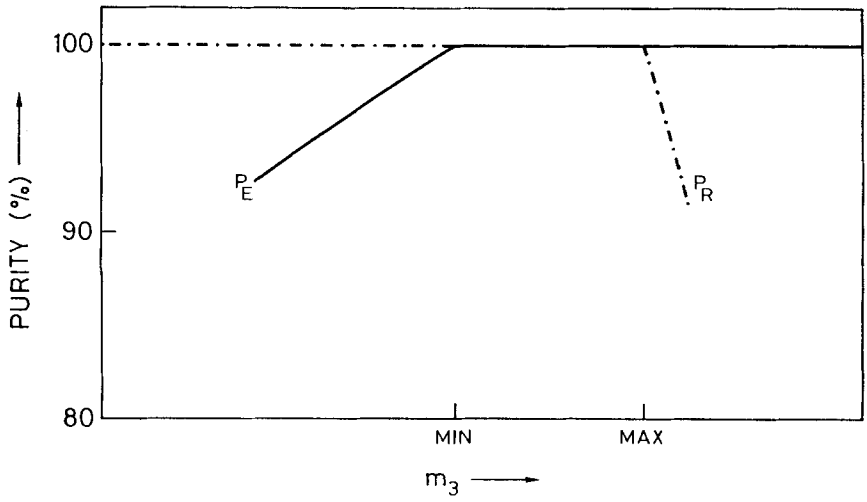

FIG. 15. Extract (P_E) and raffinate (P_R) purity values as a function of the mass flow rate ratio in Section 3 as predicted by the Equilibrium Theory.

valve switch. This results in the presence of *p*-xylene in both the raffinate and in the outgoing desorbent. The flow rate ratio in Section 4 must be low enough to adsorb all the *m*-xylene from the fluid phase. If it is greater than its upper limit value, some *m*-xylene remains in the outgoing desorbent and, in a closed loop configuration, it will be carried to Section 1, making the extract purity drop.

This behavior is represented in Figs. 16 and 17 by the curves of extract and raffinate purity as calculated through the Equilibrium Theory. If flow rate ratios in Sections 1 and 4 are kept in the complete separation region, a change in their values affects the enrichment in the withdrawal streams. In fact, the difference between mass flow rates in Sections 1 and 4 is equal to the net desorbent flow rate: the smaller it is, the greater the enrichments in extract and raffinate are and vice versa. This effect is predicted by the Equilibrium Theory, and the results are also shown in Figs. 16 and 17 where the concentration of *p*-xylene in the extract decreases when m_1 (and consequently the net desorbent flow rate) increases, whereas the concentration of *m*-xylene in the raffinate increases when m_4 (and consequently the net desorbent flow rate) decreases.

The combined effect of m_1 and m_4, when both are chosen so as to obtain complete separation, can be seen from the experimental Runs F, H, and J in Table 2. Going from one to the next, m_1 decreases and m_4 increases, hence the net desorbent flow rate decreases monotonically. The experi-

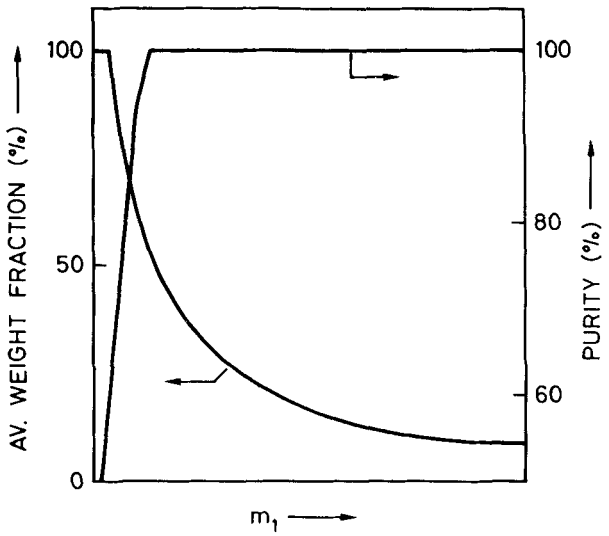

FIG. 16. *p*-Xylene average weight fraction in the extract and raffinate purity as a function of the mass flow rate ratio in Section 1 as predicted by the Equilibrium Theory.

mental results confirm equilibrium theory predictions: the concentrations of *p*-xylene in the extract and of *m*-xylene in the raffinate increase as expected while the separation remains very good. Notice that in the experimental Run H, the best performance in terms of extract and raffinate purity has been obtained.

6. CONCLUDING REMARKS

An SMB pilot plant characterized by a low number of ports (6) has been built up and operated in the vapor phase. It has been shown that complete separation can be achieved for a mixture of *m*- and *p*-xylenes using isopropylbenzene as desorbent and KY zeolites as adsorbent.

The dynamic behavior of the unit has been investigated and compared with model predictions as well as experimental results reported in the literature for a 24-port SMB pilot plant operated in the liquid phase. It has been shown that the dynamics of the SMB unit operated in the vapor phase is about four times faster than that of the corresponding unit operated in the liquid phase. This is supposed to have significant consequences on the relative economics of the two separation units.

The role of the key design parameters on the steady-state separation performance has been investigated experimentally and compared qualitatively with the predictions of the Equilibrium Theory. The results obtained

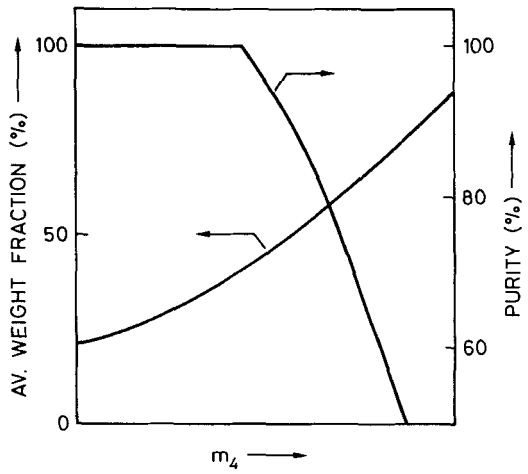

FIG. 17. *m*-Xylene average weight fraction in the raffinate and extract purity as a function of the mass flow rate ratio in Section 4 as predicted by the Equilibrium Theory.

confirm the usefulness of this simplified model in describing the unit's behavior as well as the reliability of the design equations previously developed based on this model (*9*).

Acknowledgments

We gratefully acknowledge the financial support of CNR Progetto Finalizzato Chimica Fine II. L.T.F. is thankful to CNpq and PETROBRAS/CENPES for supporting his research activity.

NOTATION

a_p	pellet external surface
c	fluid phase weight fraction
$\mathcal{D}_L$	axial dispersion coefficient
d_p	particle equivalent diameter
k	overall mass transfer coefficient
L	column length
L_j	section length, TCC unit
m_j	mass flow rate ratio in Section j
N	overall number of ports
n^{cyc}	number of cycles, $n^{cyc} = t/(Nt^*)$
n_j	number of ports in Section j, SMB unit
n^*	number of port switches, $n^* = t/t^*$
P_E	extract purity, $P_E = c_{p\text{-X}}/(c_{p\text{-X}} + c_{m\text{-X}})$

P_R raffinate purity, $P_R = c_{m\text{-}X}/(c_{p\text{-}X} + c_{m\text{-}X})$
Pe Peclet number, $\text{Pe} = ud_p/\mathcal{D}_L\epsilon$
St Stanton number, $\text{St} = k a_p L\epsilon/u$
t^* switching time
t_{ss} time to reach cyclic steady-state
u_j superficial fluid phase velocity in Section j, TCC unit
u_j^* superficial fluid phase velocity in Section j, SMB unit
u_s superficial solid phase velocity
Γ^∞ adsorbed phase saturation concentration
ϵ external void fraction
ϵ_p intraparticle void fraction
ρ_f fluid phase density
ρ_s bulk solid mass density

REFERENCES

1. D. M. Ruthven, *Principles of Adsorption and Adsorption Processes*, Wiley, New York, 1984.
2. D. B. Broughton and C. G. Gerhold, "Continuous Sorption Process Employing Fixed Beds of Sorbent and Moving Inlets and Outlets," U.S. Patent 2,985,589 (May 23, 1961).
3. H.-K. Rhee, R. Aris, and N. Amundson, "Multicomponent Adsorption in Continuous Countercurrent Exchangers," *Philos. Trans. R. Soc. London, A269*, 187 (1971).
4. D. M. Ruthven and C. B. Ching, "Counter-current and Simulated Counter-current Adsorption Separation Processes," *Chem. Eng. Sci., 44*, 1011 (1989).
5. G. Storti, M. Masi, and M. Morbidelli, "On Countercurrent Adsorption Separation Processes," in NATO ASI *Adsorption: Science and Technology* (A. E. Rodrigues et al., eds.), Kluwer Academic Publishers, 1989.
6. G. Storti, M. Mazzotti, L. T. Furlan, and M. Morbidelli, "Operation and Design of a Four Port Switching Adsorption Separation Unit," in *Adsorption Processes for Gas Separation* (F. Meunier and M. D. LeVan, eds.), (Collection *Récent Progrès en Génie des Procédés), 17* (1991).
7. B. Balannec and G. Hotier, "From Batch Elution to Simulated Counter-current Chromatography," in *Preparative and Production Scale Chromatography with Applications* (G. Ganetsos and P. E. Barker, eds.), Dekker, New York, In Press.
8. H.-K. Rhee, R. Aris, and N. Amundson, *First-order Partial Differential Equations*, Vol. II, Prentice-Hall, Englewood Cliffs, New Jersey, 1989.
9. G. Storti, M. Masi, S. Carrà, and M. Morbidelli, "Optimal Design of Multicomponent Adsorption Separation Processes Involving Nonlinear Equilibria," *Chem. Eng. Sci., 44*, 1329 (1989).